Aerobiologia (2005)
DOI 10.1007/s10453-005-9001-z
© Springer 2005

Transport efficiency and deposition velocity of fluidized spores in ventilation ducts

Paula Krauter[1,*], Arthur Biermann[1] & Lloyd D. Larsen[2]
[1]*Lawrence Livermore National Laboratory, 7000 East Ave., Livermore, CA 94550, USA;* [2]*West Desert Test Center, U.S. Army Dugway Proving Ground, Dugway, UT 84022, USA;*
*(*Author for correspondence: Phone: +1-925-422-0429; Fax +1-925-422-2095; E-mail: krauter2@llnl.gov)*

(Received 7 September 2004; accepted 17 June 2005)

Key words: *Bacillus atrophaeus*, *Bacillus globigii*, biological warfare agent, fluidized spore, spore deposition, spore transport, ventilation duct

Abstract

Experiments with dry, fluidized spores were conducted in a test apparatus to delineate the extent of spore contamination and deposition behavior under normal airflow conditions within a ventilation system. The surrogate biological warfare agent used in experiments was the spore-forming bacterium *Bacillus atrophaeus*. Viable-spore-counting methods were used in the study because they provide the most important number for estimating human health effects. Three common ventilation duct materials were evaluated: flexible plastic, galvanized steel, and internally insulated fiberglass. Transport efficiency ranged from 9 to 13% in steel and fiberglass ducts; transport efficiency was far less (0.1–4%) in plastic duct. Results showed that the deposition of surrogate biological warfare agent was significantly different in the three duct materials evaluated. All experimentally determined, dimensionless deposition velocities were in the range of theoretical predictions for dimensionless roughness, $k^+ = 10$. All were 10–100 times greater than the velocities predicted for ducts with smoother surfaces, $k^+ = 0.1$. For plastic duct, greater dimensionless deposition velocities were likely the result of charge forces between spores and surface. However, for the steel duct, a relatively large dimensionless deposition velocity was unexpected. These findings imply that building contamination will likely vary, depending on the specific type of duct material used throughout an affected area. Results of this study may aid in refining existing particle-transport models and remediation activities.

Abbreviations: ANOVA – Analysis of variance; APS – Aerodynamic particle sizer; *B. anthracis* – *Bacillus anthracis;* BG – *Bacillus globigii (B. atrophaeus);* BWA – Biological warfare agent; C – Coulomb; CFU – Colony forming unit; C_s – Cunningham slip factor; D – Duct diameter; d – Particle diameter; HEPA – High-efficiency particulate air (filtration system); HVAC – Heating, ventilating, and air conditioning (system); k^+ – Dimensionless roughness; L – Duct length; PB – Phosphate buffer; PBS – Phosphate-buffered saline; R_e – Reynolds number; RH – Relative humidity; SD – Standard deviation; TSA – Trypticase soy agar; V_d – Particle deposition velocity; U_a – Velocity in the duct; η – Kinematic viscosity; u^* – Friction velocity; ρ – Particle density; τ – Particle relaxation time; v – Viscosity

1. Introduction

Despite the rapid evolution of decontamination technologies for use against biological warfare agents (BWAs), important questions remain unanswered concerning the dispersion, deposition, and reaerosolization of weaponized spores in heating, ventilating, and air conditioning (HVAC) ducts. Building ventilation ducts are a means to contaminate a building and the surrounding area. Understanding the physical properties of ducts and their effects on spore dispersion can help architects design HVAC systems that can maximize occupant safety. Understanding spore deposition in ventilation ducts can help facility managers to reach informed decisions about how to modify existing ventilation systems for improved security and can enhance the calibration of indoor particle-deposition models.

Aerosolization may be the most dangerous method of BWA dissemination because of the potential for rapid spread of agent throughout a building and the difficulty in detecting the agent (Kowalski, 2002). Between October 2 and November 2, 2001, anthrax spores were disseminated from letters mailed through the U.S. Postal Service (Atlas, 2001). Subsequent cleanup of the Hart Senate Office Building in Washington DC cost more than $26 million. A member of the decontamination task force stated that spore reaerosolization was an important factor during cleanup and a possible reason that three cycles of chlorine dioxide fumigant were required in some locations (Weis et al., 2003). However, certain duct materials themselves may aid in building restoration by decreasing the potential for spore reaerosolization and transport.

A comprehensive literature review (Sippola, 2002) revealed that considerable experimental data regarding particle deposition from turbulent flows has been collected using a range of techniques of varying quality (Sippola and Nazaroff, 2002). According to the authors, models can capture broad trends seen in experiments, but modeled results can deviate markedly from observations. Much of the published research predicts particle-deposition rates based on empirical equations, Eulerian models, sublayer models, and Lagrangian simulations. The existing modeling approaches and empirical data may not be sufficient to reliably predict particle deposition in ventilation ducts. Obtaining accurate data for predicting particle deposition rates is a concern regardless of the type of predictive method used.

Previous investigations have quantified the deposition of particles, using experimental and theoretical studies of indoor aerosols, including factors such as airflow from room to room and deposition on interior surfaces (Wallace, 1996; Lai and Nazaroff, 2000; Sextro et al., 2002; Thacher et al., 2002). Our investigation focuses on bacterial endospore deposition in common ventilation duct materials – specifically, flexible plastic, galvanized steel, and internally insulated fiberglass – by quantifying culturable airborne spores in the air fraction and on duct surfaces. A dry powder of fluidized spores, predominately 1-μm-diameter particles, is expected to float and stay aloft longer than larger spore clumps in nonfluidized spore preparations (Matsumoto, 2003). In this study, several methods were used to sample the air fraction and surfaces of ducts for culturable spores. Culturable spores were enumerated from commercially available duct surfaces by surface-sample techniques and from the air fraction by impingers. Electrostatic, moisture, and thermal measurements were also made because of their influence on deposition velocity. To our knowledge, no other published report has analyzed the deposition of dry, fluidized spores under these experimental conditions to determine surrogate BWA transport efficiencies and deposition velocities.

2. Methods

2.1. *Experimental apparatus*

The test apparatus consisted of 15.2-cm-diameter ducting divided into three sections that were a total of approximately 13.7 m long. As shown in Figure 1, the apparatus included four bends of approximately 90° each, two 2-m vertical rises, and 10 m of horizontal duct.

A vacuum blower drew air into section 1 of the test apparatus, through a high-efficiency particulate air (HEPA) filtration system, and into a 2-m section of galvanized steel duct. A modified Stairmand air mixer was place within the proximal end of the duct to ensure turbulent airflow. An anemometer (Kurz, Series 2440, Monterey,

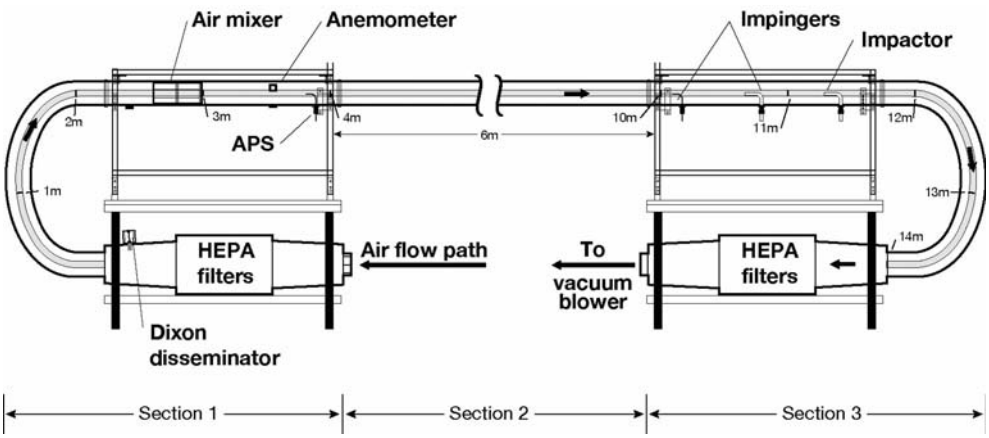

Figure 1. The test apparatus consisted of 15 cm^2-diameter duct with four 90° bends and two 1–5 m vertical rises. The horizontal section (section 2) was 9.1 m long but could be expanded to any length. Intake air was HEPA filtered, and the airflow was mixed with a modified Stairmand air mixer. Several isokinetic probes with pumps were placed in the air duct for measurement purposes. Airflow was 2.83 m^3/min; velocity was 2.6 m/s. Air was exhausted though a second HEPA filter located in section 3 of the apparatus. Surface samples were taken from the mid-point to the end of section 2.

CA) attached to a personal computer logged the airflow. Airflow through the duct was balanced to 2.83 ± 0.05 m^3/min, a flow rate typical in ventilation ducting of this size. The turbulent airflow velocity profile in the 15.2-cm-diameter duct was measured 3.05 m from the spore release point (Dixon disseminator) with an anemometer.

Spores were introduced into the airflow using a Dixon disseminator. The disseminator was a metal chamber containing a measured weight of spores and attached to a port on the duct system. The disseminator contained a diaphragm that ruptures under an external pulse of pressurized air, resulting in the near-instantaneous release of spores into the duct system. Air pressure was exerted in the chamber, resulting in a dispersion of spore powder into the duct airstream. The target value for spore deposition densities was in the range of 10^7 colony-forming units (CFU) per 25 cm^2 of sample area. Release of spores into the duct did not perturb the airflow above normal operational fluctuations. Aerosol particles were characterized by an aerosol particle sizer (APS Model 332000, TSI, Maplewood, MN) located in section 1 of the test apparatus. Section 1 also included an all-glass impinger (Aces Glass, Inc., model 7540, AGI-30) with an intake velocity that is internally limited by a critical orifice to 12.6 L/min (STP). A 1-min air sample was withdrawn from the duct system via the impinger into 17.5 ml of phosphate-buffered saline (PBS). Samples were mixed, serially diluted, vortexed, plated onto trypticase soy agar (TSA), and incubated for 24 h at 37 °C.

Section 2 of the test apparatus contained a removable 6.1-m section of duct. Three duct materials were tested in this study. The first material was flexible plastic (Master Flow, R-6.0 insulated, two-layer core of polyester film that encapsulates a galvanized wire helix, L.L. Building Products Inc.). The second material was galvanized (zinc-coated by the hot-dip process) steel (L.L. Building Products Inc.). The third material was internally insulated fiberglass (proprietary acrylic polymer interior surface coating, Air Duct MH-12358, Johns Manville, SuperRound®). The plastic and galvanized steel ducts had smooth internal surfaces; the fiberglass duct had a rough internal surface (Table 1). Because of duct seams and connections, and the wire helix in the flexible plastic duct, internal macrosurfaces were not smooth. The 6-m section of duct was used for collecting spores that had settled onto the internal duct surfaces.

Section 3 of the apparatus was a 2-m length of galvanized ducting equipped for air sampling. This section was instrumented with two impingers and an Andersen Impactor (Thermo Andersen, Smyrna, GA). Each instrument was on a separate, rotary-vane pump set to the manufacturers' recommended flow rate. Results from the Andersen viable 6-stage impactor provided estimates of

Table 1. Duct descriptions and roughness measurements

Duct material	Duct description	Roughness height[a] (mm)
Flexible plastic	Smooth, two layers of polyester film encapsulating a galvanized steel wire helix; multiple 0.1- to 0.3-cm folds	0.005[b] ± 0.002
Galvanized steel	Smooth, steel sheet, galvanized with a zinc coating; a thin film of corrosion forms when exposed to the atmosphere	0.15[b] ± 0.05
Fiberglass	Rough, internal fiberglass wool insulation on board coated with acrylic polymer and a protective agent to protect coating from potential growth of fungus and bacteria	1.5 ± 0.9

[a]Difference between the highest and lowest points within the sampling length.
[b]Information from manufacturer and Internet search.

aerosol concentration and aerodynamic size distribution. The impactor vacuum pump was adjusted to a flow rate of 28.3 L/min. Sampling time was the duration of five air exchanges. Spores were collected on TSA plates for all six impactor stages, incubated, and counted according to a published procedure (ThermoAndersen).

The Aerodynamic Particle Sizer (APS) included an internal pump that produced a sample flow rate of 1 L/min. Air flow through the test duct was exhausted through a second HEPA unit. Isokinetic probes and rotary vane pumps that supported the test apparatus were able to accommodate a variety of testing configurations. Temperature and humidity during each test were monitored.

2.2. *Spore surrogate*

The surrogate organism for *Bacillus anthracis* was the spore-forming bacterium, *B. atrophaeus*, also known as *B. globigii* (BG). BG is a gram-positive, durable, spore-forming bacterium that is common in certain soils, noninfectious, easily grown in culture, and easily detected. The BG used in this study was a dry powder (2.33×10^{11} spores/g) that was characterized by scanning electron microscopy and by a 6-stage, viable, Andersen impactor and an APS for aerodynamic size in the aerosol state. Dried spores were prepared and characterized by scientists at Dugway Proving Ground, Dugway, Utah. Spores ranged from 0.6 to 1.1 μm in three separate analyses. Fluidized spores are reasonable facsimiles of weaponized spores.

2.3. *Spore deposition on duct materials*

Fluidized BG (a recognized simulant for some BWA's, 0.07–0.10 g) was introduced into the turbulent airflow (2.83 m^3/min) of the test apparatus. A portable thermal anemometer installed in the duct measured and recorded air velocity for each test. The Reynolds number (R_e 26,000) reflected airflow within the lower region of turbulence. Initial dispersal of BG spores ranged from approximately 7×10^9 to 1×10^{10} spores.

After spore dissemination, air samples were collected while five volumes of air were exchanged. After the exchange of five air volumes within the duct, the test apparatus was shut

down. After 30 min surface samples were then collected on the inside surfaces of the ductwork using a predefined sampling grid. Ductwork for section 2, the second 3-m length of duct, was sampled using wet swabs (Puritan Medical Products, Co., Guilford, ME) at the top, bottom, right, and left sides every 30–38 cm.

Data collected during each test included air velocity, temperature, relative humidity, spore counts in air, APS size distribution profiles, Andersen impactor size analysis, and spore counts on interior duct surfaces using wet-swabs on surfaces and by total immersion and bacterial enumeration of physically excised sections of ductwork.

2.4. *Duct surface samples*

Surface samples were collected from the second half of the duct, located in section 2 of the apparatus (see Figure 1). The size of each surface sample area was 25 cm^2. A 5.1-cm by 5.1-cm area is recommended for environmental and medical device sampling in the *Clinical Microbiology Procedures Handbook* (Gilchrist, 1992). For each of nine locations at approximately 30- to 38-cm intervals along the duct, four samples were collected: at the bottom, left side, right side, and top of the duct. Sterile polyfiber-tipped swabs (Puritan Medical Products, Co., Guilford, ME) were moistened with sterile PBS solution and rolled vertically and horizontally within a 25-cm^2 area of duct. Sample areas were identified by a clean Teflon sample template used to delineate sample-collection boundaries. Swabs were then placed in a test tube containing 10 ml of PBS with 0.1% TritonX-100 (Sigma) and mixed for 10 min on a wrist action shaker. Samples were serially diluted, vortexed, and plated on TSA (ATCC Medium 18) in triplicate and incubated at 37 °C for 24 h. Other authors have studied the efficiency of the standard swab sampling method (Sanderson et al., 2002; Rose et al., 2004). This study is evaluating the difference among treatments and not evaluating the sampling technology.

For rough-surface ducts, 25-cm^2 sample coupons were cut from the internal surface of the duct, separating the internal surface from the fiberglass insulation. The coupons were placed in 20 ml of sterile phosphate buffer and sonicated for 10 min. These samples were treated in the same manner as the wet-swab samples. Additional coupon samples were cut from galvanized steel and flexible plastic as a quality-assurance measure for the surface-swab-sampling technique used on smooth-surface ducts. The external surfaces of the plastic and steel coupon samples were cleaned with ethanol and dried, and the duct coupon was processed in the same manner used for fiberglass duct. Field blanks comprised approximately 10% of the total number of samples.

2.5. *Static measurements*

Static measurements were obtained using a JCI 140 Static Monitor and Faraday pail (John Chubb Inst., Unit 30, Cheltenham, England). The measurement quantifying charged materials was in coulombs (C). The level of detection for the measurement was 0.01 nC. Galvanized steel duct samples were grounded; whereas, plastic and fiberglass samples were not grounded because those materials do not conduct an electrical charge.

2.6. *Standardized negative controls*

Controls were run with manipulations similar to those for the samples of contaminated duct surfaces. Five percent of the samples were method blanks (1:20 samples). Background counts were assessed after a total of ten air exchanges had passed through the ducts for each duct material tested. Airflow was turned on for five air exchanges, turned off for a rest period of 15–30 min, and turned on for another five air exchanges. The impingers were sampled and analyzed for total microbial counts using Standard Method 9215 (Clesceri et al., 1989). After each test set, sterile impingers with sterile media were reconnected to the appropriate probes. No BG was found on any of the three duct materials tested prior to BG release.

2.7. *Statistical analysis*

Data were logarithmically transformed to best represent the central tendency of the data. Once the results were transformed, further tests could be based on the assumption that the data were sampled from a Gaussian population. The BG

counts from each test were compared to those for all other tests. The analysis of variance (ANOVA), a comparison of the means and deviations of all tests, was conducted.

Further statistical testing was conducted following ANOVA to determine which data sets were significantly different from each other. The Bonferroni Multiple Comparisons Test was used to reduce the overall chance of a spurious significant difference and to ensure that there was a 95% chance that differences between the data were within the calculated confidence intervals.

3. Results

3.1. *Environmental conditions during tests*

Environmental conditions, such as relative humidity (RH) and air temperature, were monitored but not regulated during tests. Testing took place inside a decommissioned building at Dugway, Utah, that was not temperature controlled. The RH was typical of normal fluctuations found in high-desert conditions and ranged from 9.0 to 39.9%. During spring tests, the mean RH of intake air was 24.3% (SD ± 9.8); the mean RH of exhaust air was 23.6% (SD ± 9.9). During summer tests, the RH ranged from 19.3 to 36.9%, with an average RH of 26.1% (SD ± 6.1). The relatively high RH was due to a thunderstorm weather pattern. During spring tests, the temperature of intake air ranged from 9.6 to 15.7 °C (average = 13.2 °C $\pm$ 2.2). During summer tests, air-intake temperatures ranged from 25.5 to 31.4 °C (average = 28.7 °C $\pm$ 1.0).

Aerosol background spore counts were assessed periodically during each test period. The HEPA-filtered air flowing into the test apparatus had nondetectable (<1 CFU/L air) spore counts during both test periods. Impinger (AGI) background data for all types of microorganisms capable of growing on TSA at 37 °C ranged from 1.2 to 2.4 CFU/L of air (average = 2 CFU/L).

Ducts were purchased commercially and were not precleaned or treated aseptically. The average background microbial count for all types of aerobic bacteria in the ducts was 40 ± 12 CFU/cm^2 for flexible plastic, 32 ± 8 CFU/cm^2 for galvanized steel, and 108 ± 4.4 CFU/cm^2 for fiberglass duct. The detection level for this analysis was 1 CFU/cm^2. The background number of BG on duct surfaces was below the detection level. BG colonies have a distinct persimmon orange pigmentation that allows them to be easily distinguished from native flora. Non-pigmented, background microbial counts were significantly less than those for each of the six BG spore-deposition tests (for all tests, $p < 0.001$). Data from each replicate test on flexible plastic, galvanized steel, and fiberglass duct were logarithmically transformed to best represent the central tendency of the data. Multiple comparison tests were conducted to ensure a 95% chance that the differences between all population means lay within the calculated confidence intervals. The one-way ANOVA p value was significant ($p < 0.0001$). Bonferroni multiple comparison post-tests between the six deposition tests and the background test were conducted to determine which data sets differed.

3.2. *Turbulent airflow profiles*

An anemometer measured the airflow during each test. Release of spores into the airstream did not perturb the airflow of the duct system beyond normal operational fluctuations according to anemometer measurements. Tests were run at a velocity of 2.6 m/s. This velocity is within the air speed range typically found in ventilation ducts (2–9 m/s). The Reynolds number was 26,000 placing the airflow in the range of turbulent airflow.

The turbulent airflow profile in the 15.2-cm-diameter duct (Figure 2) was measured with the anemometer across the duct at 3-m and 10-m downstream from the spore-release location. Measurements were from the bottom of the duct to the top. Air velocity declined from 35 to 100 cm/s near duct walls when measured 10 m from the source. Air velocity adjacent to the duct walls was about 40–85 cm/s less than airflow within the center of the duct (315–330 cm/s) when measured 3 m from the source. Velocity profiles in the test apparatus followed the Prandtl one-seventh power law describing turbulent flow (FM-WebBook).

3.3. *Aerosol characterization and distribution*

The spore preparation used in this study was characterized by the APS, 6-stage Anderson impactor and scanning electron microscopy (Figure 3). The spore preparation shown in

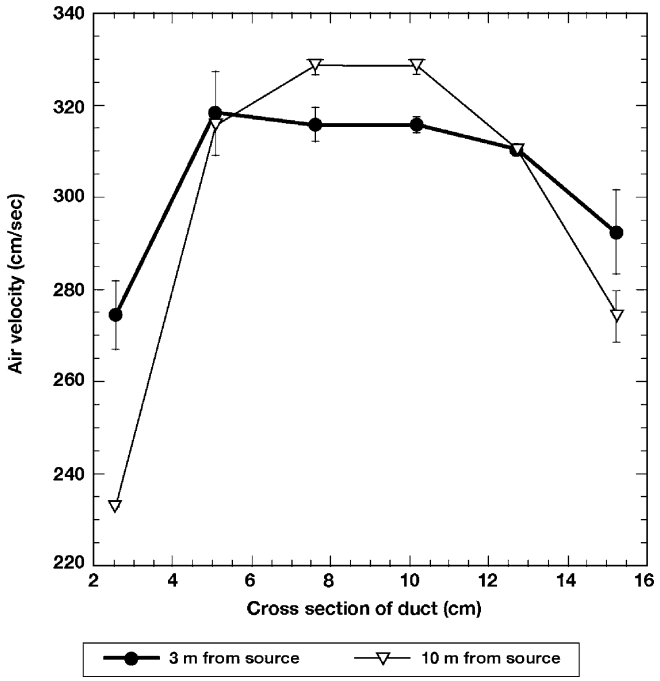

Figure 2. Turbulent airflow profiles in 15.2 cm-diameter duct 3 m and 10 m downstream from the spore release location. Measurements are from the bottom of the duct to the top. Airflow declined by about 0.007 m^3/s near the duct walls. Error bars show the standard deviation (SD) of the data.

Figure 3 consists of irregular clusters of small particles. Most spores used during tests were single particles, ellipsoidal in shape and about 1 μm in diameter.

Most airborne particles evaluated in the Anderson impactor, which was located 11.5 m downstream from the point of release, were 0.65–3.3 μm in diameter. Viable or culturable background airborne particles tended to be slightly larger (27% of the microorganisms were 3.3–4.7 μm in diameter) than the BG spores released from the disseminator. The background airborne microbial count in ventilation ducts was, on average, 2 CFU/L air. Initial release of spores into the duct resulted in an airborne contaminant load of 10^4–10^6 viable spores/L of air after traveling about 10 M in the duct apparatus to reach the impinger samplers.

Figure 4 is an example of the APS spore size distribution from a test conducted in late summer. The peak distribution of aerosol particles was at about 1.0 μm in size. The entire size distribution ranged from 0.55 to 9 μm.

A test using the disseminator showed that the spore plume moved through the ventilation duct in about 25 s (Figure 5). Spores traveled through a 2-m rise and two 90° bends to travel past the isokinetic probes and APS system located 3.5 m downstream from the spore-release location. These data suggest that the spore plume was generally limited to a finite time frame of several seconds.

Variability was observed in spore dissemination using the Dixon disseminator. Spores were released into the duct under positive air pressure, but when the six deposition tests were compared, results from one test on flexible plastic duct showed poor dissemination of spores. The APS data suggest a variation in the spore-dispersal mechanism during this test as the cause, resulting in a ten-fold decrease in particle counts (Table 2). Spores disseminated in the flexible plastic duct resulted in a relatively small number of particles during this test, and a correspondingly small number of viable spores were found in the impinger samples from that test. The percent of culturable spores recovered from the aerosol samplers was about 5–7% for plastic duct, and ranged from 20 to 24% for tests using galvanized steel and fiberglass duct. Particles other than spores counted by

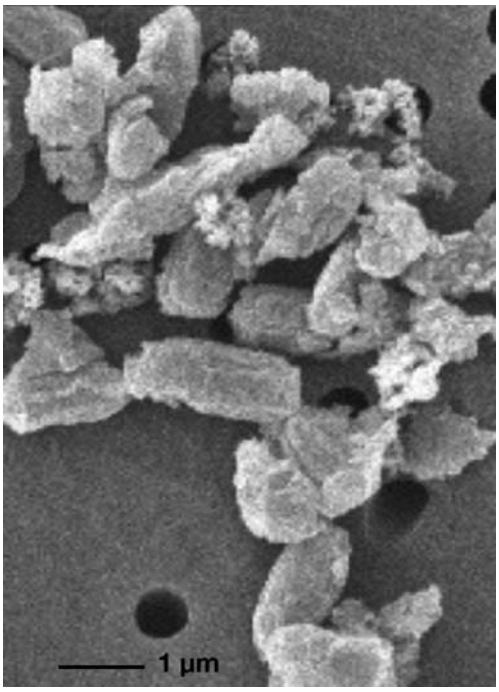

Figure 3. Scanning electron micrograph (4000×) of the *B. atrophaeus* spore preparation.

the APS may include fragments of spores, production materials, and particles lifting off the duct or internal surfaces of the test apparatus.

3.4. *Fluidized spore deposition onto ventilation ducts*

Uniform collection of spores from duct surfaces was difficult because the ducts tested included both smooth and rough surfaces. Thus, recovering spores deposited onto surfaces of the different duct materials required two sampling techniques. Coupon samples (a 25 cm^2 section cut from the top, sides, and bottom of duct) were treated as a subset of the smooth duct surface samples and were the sole surface sample technique used for fiberglass duct. Some coupons were also collected from the plastic and steel duct surfaces. When comparing the differences between plastic and steel coupon samples ($n=8$ for each duct type) versus swab samples ($n=72$ for each duct type), there was no significant difference between the data sets (Table 3). Because all surface samples from the fiberglass duct were coupon samples ($n=40$), they were not included in this comparison.

Data on spore surface deposition was the combination of data from the two tests from each duct material. Each duct type was sampled several times down the length of the duct at the top, sides, and bottom. The means and standard

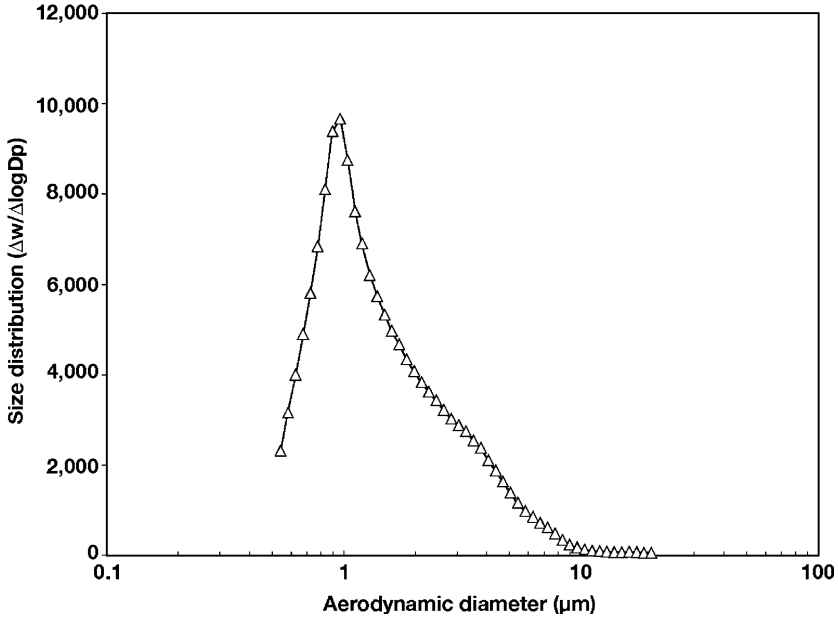

Figure 4. Spore size distribution. Spores introduced into the duct with a Dixon disseminator were analyzed using an aerosol particle sizer. The aerosol consisted of particles predominantly 0.6–1.1 μm in size.

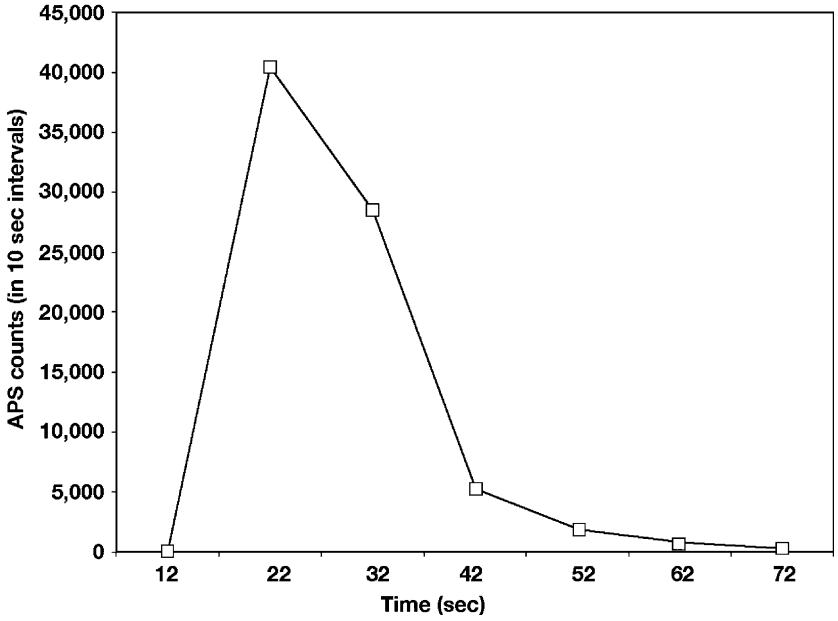

Figure 5. Spore dissemination measured over 10 s intervals by the APS.

Table 2. Aerosol particle counts during the test (aerosol particle counter) and viable spore counts (standard culture method) in aerosols

Duct material	Dry spores released (g)	Particle count (number /cm^3)	Spore concentration in aerosol (average CFU/cm^3)	Viable spore concentration in aerosol (%)
Plastic	0.09	1178	77.3	6.6
	0.10	113	5.79	5.1
Steel	0.10	4809	949	20
	0.10	3570	762	21
Fiberglass	0.07	4200	1010	24
	0.10	4330	1010	23

deviations of all data combined show relatively large variability in the data set (Table 4).

Normalized spore counts deposited in ducts from about 7 to 10 m downstream of the spore-release location were different for plastic compared to steel and fiberglass (Figure 6). Normalized surface-spore counts were in the range of $10–10^3$ CFU/cm^2 in each of the three duct materials tested. Data in Figure 6 were normalized by dividing the average number of viable spores obtained from surface samples, by the average number of airborne viable spores from impinger samples. This calculation essentially factors out the variability of the spore dissemination device to eliminate skewing of the surface counts. The flexible plastic duct had about ten-fold greater

Table 3. Comparison of logarithmically transformed data from counts collected from coupons and swab samples using an unpaired Student *t*-test and Welch *t*-test

Duct type/sample method	Number (n)	Average CFU per cm^2 sample	Unpaired Student *t*-test Wet Swab vs. Coupon (p value)	Alternate Welch *t*-test[a] Wet Swab vs. Coupon (p value)
Plastic/swab	72	9.31×10^5	0.93	0.92
Plastic/coupon	8	6.17×10^5	–	–
Steel/swab	72	7.38×10^5	0.67	0.52
Steel/coupon	8	3.03×10^5	–	–

CFU counts were combined from replicate tests. The p values are insignificant (>0.05).
[a]Unequal standard deviations of transformed data.

Table 4. Means and standard deviations (SDs) of normalized spore-deposition data in three duct materials

Duct material	Number (n)	Normalized surface concentration to air [(number/cm^2)/(number/cm^3)]			
		Mean	Standard deviation	Average test 1	Average test 2
Plastic	72	917	640	927	70
Steel	72	35	28	19.5	44.5
Fiberglass	40	9.8	4.9	8.6	9.7

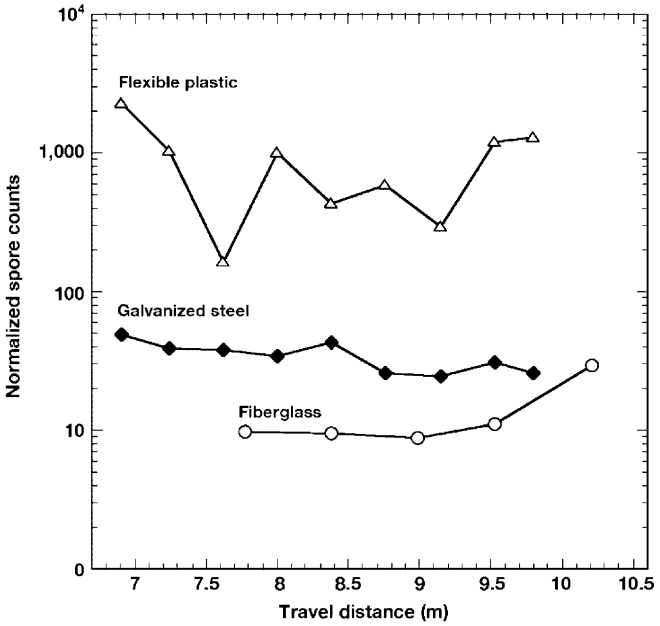

Figure 6. Combined data showing normalized (spores on surfaces/spores in aerosol), average spore counts from the top, sides, and bottom of ventilation ducts. Each duct type was tested twice. Error information is given in Tables 4 and 5.

surface spore counts compared to counts for galvanized steel and fiberglass ducts.

Table 5 shows results of the ANOVA test for the log-transformed, surface-deposition data. The one-way ANOVA to compare the three duct materials resulted in a p value for coupon samples of < 0.001. Therefore, Bonferroni Multiple Comparisons tests were conducted to determine the difference between the tests. Spore deposition on flexible plastic duct was significantly different compared to steel duct ($p < 0.001$) and fiberglass ($p < 0.001$). There was no significant difference between spore distribution counts on steel and fiberglass ducts.

Fluidized spores were not, in all cases, deposited on duct surfaces as we had predicted, with the largest numbers falling to the bottom of ducts and fewer adhering to the top of ducts. Over a distance of about 7–10 m, spores were deposited

Table 5. Bonferroni multiple comparisons test of spore counts from surface samples from three duct materials

Comparison	p value	Lower 95% confidence interval	Upper 95% confidence interval
Plastic vs. steel	$p < 0.001$	494	1270
Plastic vs. fiberglass	$p < 0.001$	349	1268
Steel vs. fiberglass	$p > 0.05$[a]	−533	386

Dividing surface counts by aerosolized counts normalizes the surface spore count data. Data were logarithmically transformed.
[a]Not significant.

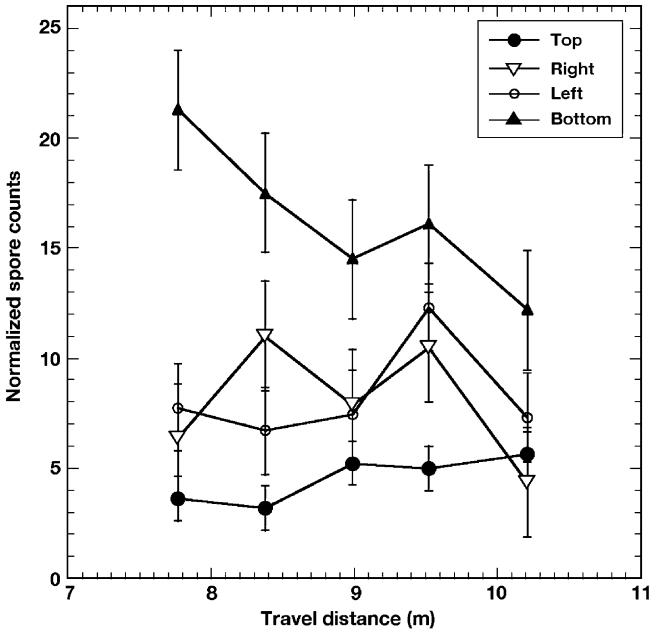

Figure 7. Viable spore counts on fiberglass duct surface after five air exchanges at an airflow of 2.83 m^3/min.

predominantly on the bottom and sides of the fiberglass duct (Figure 7). However, in the galvanized steel duct, more spores deposited on the bottom and right side of the duct than on the top and left side (Figure 8). This result may be a consequence of the horizontal joint running the length of the duct. Spore deposition on plastic duct was extremely variable from location to location (data not shown). Some researchers have suggested that particles do not settle onto the top

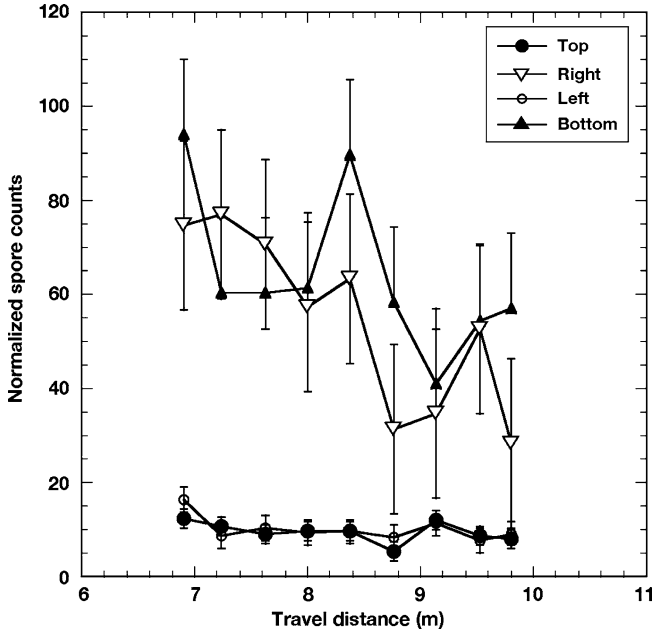

Figure 8. Viable spore counts on steel duct surface after five air exchanges at an airflow of 2.83 m^3/min.

Table 6. Aerosol-only dissemination efficiency[a] and total dissemination efficiency[b] in three duct materials

Duct material	Aerosol dissemination efficiency (%)	Total dissemination efficiency (%)	
		Wet swab sample	Coupon sample
Plastic	1.0	5.4	3.9
	0.1	0.09	0.12
Galvanized steel	11	14	12
	9.0	10.0	9.4
Fiberglass	12	Not applicable	13
	12	Not applicable	13

Transport efficiency is defined as the total dissemination efficiency.
[a]From aerosol concentration data.
[b]From aerosol plus surface concentration data.

(ceiling) of horizontal ducts (Schmel, 1973). We found spores on all duct surfaces tested, including top, sides, and bottom. In another study with a friction velocity of 12 cm/s, ceiling deposition was observed (Sippola, 2002).

A regression analysis was conducted to determine if spore deposition declined with distance traveled in the segment of duct sampled in these tests (7–10 m from the spore-release site). A comparison of surface-spore depositions at increasing distances from the spore release point showed no differences over the length of duct tested. There was no linear trend of decreasing spore concentrations over the 3 m length of duct sampled, and no decrease in spore deposition concentration with length was seen in any of the three duct materials tested.

3.5. *Dissemination efficiency*

Table 6 shows the total dissemination efficiency and aerosol-only dissemination efficiency. Transport efficiency is defined in this study as the total dissemination efficiency. Values were calculated as follows:

$$\text{Total dissemination efficiency} = 100\frac{T_A + T_S}{T_E}, \tag{1}$$

where T_A is the total CFU passing through as aerosol, T_S is total CFU surface deposition, T_E is total CFUs in the powder preparation, and

$$\text{Aerosol-only dissemination efficiency} = 100\frac{T_A}{T_E}. \tag{2}$$

We anticipated about a 10% aerosol dissemination efficiency in the ventilation duct system. Of the six tests involving spore dissemination, one spore release into flexible plastic did not adequately disperse the material. Both the APS particle counts and AGI variable spore counts measured during the second plastic duct test suggest a poor release of spores into the test apparatus. The test resulted in an aerosol-only dissemination efficiency of 0.1%. The remaining five tests resulted in the predicted total dissemination efficiency ranges (about 4–13%). The aerosol-only dissemination efficiency in flexible plastic duct was 1.1% and 0.1%; that for galvanized steel was 11% and 9%; and that for fiberglass duct was 12%.

3.6. *Duct physical properties influencing spore deposition*

The physical attributes of duct materials that affect spore deposition include porosity of the duct material and the grade of roughness. Macro and microstructures of internal surfaces of the ducts contribute to the grade of roughness. The plastic and steel materials tested have smooth internal surfaces; however, the flexible plastic duct encapsulates a galvanized steel wire helix and contains multiple folds in the plastic film. Whereas the microstructure of plastic duct may be described as smooth (Table 1), the macrosurface of flexible plastic is rough. In addition, the horizontal joint seam in the galvanized steel duct was a feature that might affect spore deposition. The acrylic-polymer-coated fiberglass had a rough internal

Table 7. Static measurement of fluidized BG spores and ducts

Material tested	Charge (nC/g ± SD)
BG spores	+31.5 ± 1.1
	+31.3 ± 1.1
Flexible plastic	−5.84 ± 0.56
	−6.29 ± 0.62
Galvanized steel	+0.01 ± 0.01
	+0.01 ± 0.01
Fiberglass	+0.015 ± 0.10
	+0.020 ± 0.08

The charge value is the mean of five measurements.

surface with a porous, uneven inner surface. The acrylic coating on the fiberglass internal surface also included a proprietary fungal and bacterial growth inhibitor, which is discussed later.

Static measurement data for powdered spores and for the interior surface of the duct materials tested is summarized in Table 7. Charge varied slightly with time, and the average of five different measurements was recorded. The flexible plastic material was negatively charged (−6 nC/g) as measured by the JCI 140 Static Monitor, whereas steel and fiberglass duct materials were neutral. The powdered spore material had a positive charge (31 nC/g) prior to fluidization. Spore aerosols used in our tests were not neutralized and most likely were charged as a function of the nature of powder dissemination.

3.7. *Dimensionless particle relaxation time and deposition velocity*

Spore deposition velocities were compared against predictions from three different particle models (Figure 9). The particle models include a free-flight model for vertical rough surfaces (El-Shobokshy and Ismail, 1979), a turbophoretic model (Wood, 1981), and a sublayer model (Fan and Ahmadi, 1995). Data used in the three models include BG spore size and density, velocity, duct dimensions, and duct surface roughness. Our spore deposition rates were bounded by all three curves in the rough ($k^+ = 10$), but not the smooth ($k^+ = 0.1$), roughness regions of the particle deposition predictions.

Our calculation for deposition of aerosols in turbulent flow is from Fuchs (1964). The fractional penetration of aerosols through a circular duct having turbulent flow is given by:

$$F_{\mathrm{p,duct}} = \exp\frac{-4LV_{\mathrm{d}}}{DU_{\mathrm{a}}}, \tag{3}$$

where V_{d} is particle deposition velocity,U_{a} is velocity in the duct, and D and L are the duct diameter and length, respectively. The fractional penetration is calculated from experimental data using the expression:

$$F_{\mathrm{p,duct}} = 1 - F_{\mathrm{c}} = \frac{1 - N_{\mathrm{c}}}{N_{\mathrm{c}} + N_{\mathrm{p}}}, \tag{4}$$

where F_{c} is the fraction collected on the walls of the duct section, N_{c} is the number of CFUs collected on the walls in the section, and N_{p} is the total number of CFUs passing through in the aerosol pulse resulting from the spore dissemination. N_{c} and N_{p} were estimated from the surface (coupon and swab) concentration and aerosol (AGI) concentration data. The deposition velocities for all ducts ranged from 0.06 to 2.44 cm/s. The average deposition velocity for plastic was 1.4 cm/s, steel was 0.16 cm/s, and that for fiberglass was 0.067 cm/s. Table 8 summarizes the results of dimensionless deposition velocities.

In comparing calculated deposition velocities with the three theoretical models, particle size and deposition velocity are often transformed to dimensionless expressions, namely, the dimensionless particle relaxation time and dimensionless deposition velocity, respectively. The dimensionless particle relaxation time is given by:

$$\tau^+ = \frac{\tau u^{*2}}{v}, \tag{5}$$

$$\tau = \frac{C_{\mathrm{s}} d^2 \rho}{18\eta}, \tag{6}$$

and where τ is the particle relaxation time, u^* is friction velocity, v is viscosity, η is kinematic viscosity, d is particle diameter, ρ is particle density, and C_{s} is the Cunningham slip factor. The dimensionless deposition velocity is given by:

$$V^+ = \frac{V_{\mathrm{d}}}{u^*}. \tag{7}$$

Finally, dimensionless roughness, k^+, is based on the effective physical roughness by:

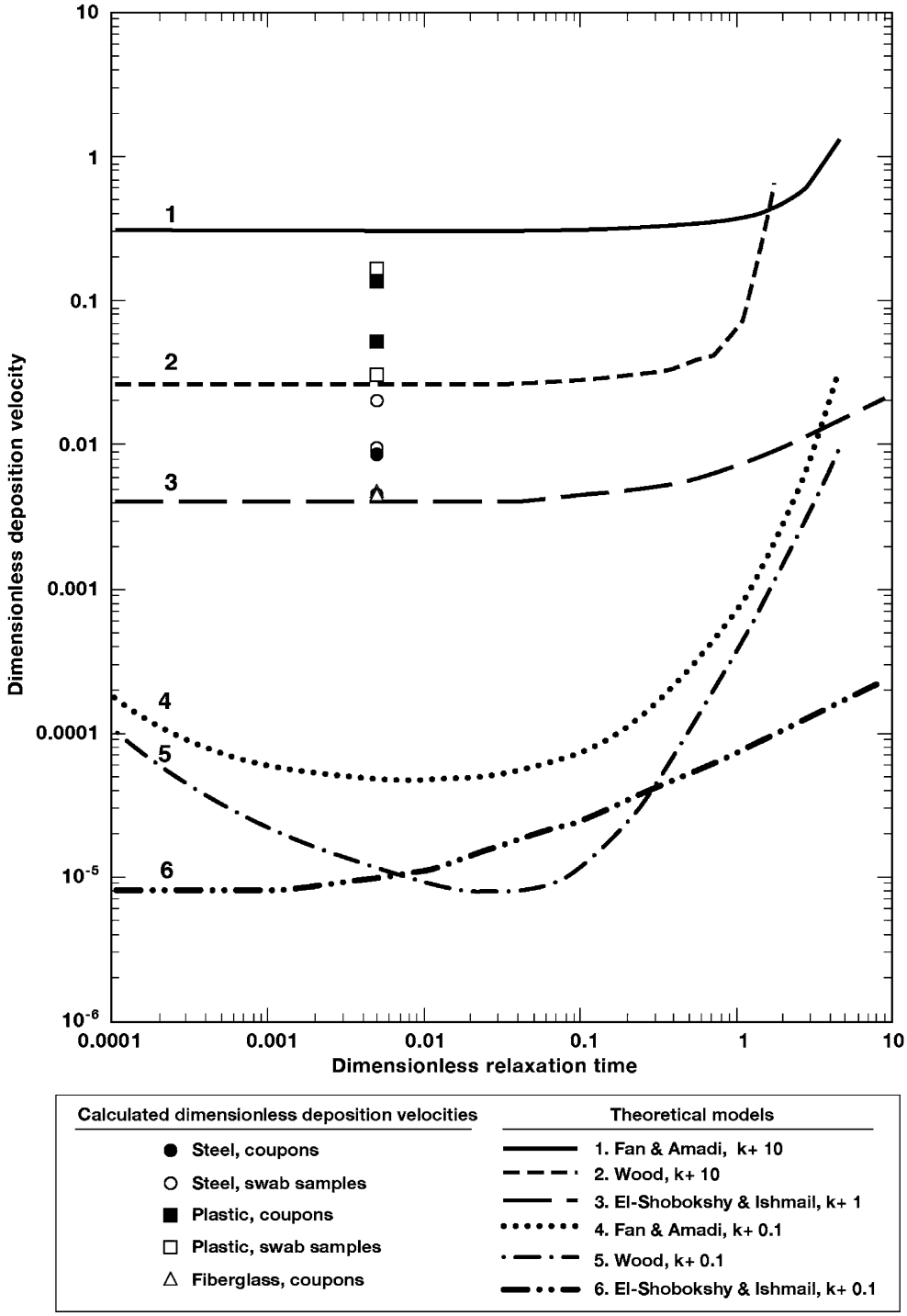

Figure 9. Calculated dimensionless deposition velocities for fluidized spores in plastic, steel, and fiberglass ducts compared with three theoretical models. The dimensionless relaxation time describing the spores was 4.9×10^{-3}.

Table 8. Deposition velocity and dimensionless deposition velocity for three duct materials

Duct material	Sample type	Deposition velocity (cm/s)	Dimensionless deposition velocity (V^+)
Plastic	Coupon	1.9800	0.13700
	Wet swab	2.4400	0.16900
	Coupon	0.7520	0.05210
	Wet swab	0.4380	0.03040
Steel	Coupon	0.1250	0.00867
	Wet swab	0.2970	0.02060
	Coupon	0.0643	0.00446
	Wet swab	0.1380	0.00957
Fiberglass	Wet swab	0.0627	0.00435
	Wet swab	0.0709	0.00491

$$k^+ = \frac{ku^*}{v}. \tag{8}$$

Estimates of effective and dimensionless roughness values are listed in Table 9 for the duct materials used in this study. The dimensionless relaxation time describing the spores in our study was 4.9×10^{-3}, and the friction velocity was 14.4 cm/s. Table 10 shows these and other parameters used in comparing our data to the theoretical models.

Table 8 shows that the greatest dimensionless deposition velocities, which ranged from 0.03 to 0.17, are for the plastic ducting. Corresponding velocities for fiberglass and steel ducts ranged from 0.004 to 0.021. As shown in Figure 9, all of our experimentally determined dimensionless deposition velocities are in the range of theoretical predictions for dimensionless roughness $k^+ = 10$. All are 10–100 times greater than the velocities predicted for ducts with smoother surfaces, $k^+ = 0.1$. As previously discussed, plastic and fiberglass ducting could be expected to have dimensionless velocities in this range because $k^+ \cong 10$–30 for the plastic macrostructure, and $k^+ = 12$ for the fiberglass. Moreover, for plastic, greater dimensionless deposition velocities might also be expected because of charge forces between spores and surface. Such forces are not accounted for in the theories. However, for the steel duct, a relatively large dimensionless deposition velocity was unexpected.

4. Discussion

Between October 2 and November 2, 2001, four or more letters containing a powdered form of *B. anthracis* were mailed through the U.S. Postal Service, resulting in the contamination of government and private facilities (U.S. EPA, 2002). According to government specialists, the geographic scope of the incidents was increased by cross-contamination of mail. Of particular concern were airflow patterns and dynamics in affected buildings and in the building ventilation systems. Such systems can become entry points or distribution systems for hazardous contaminants, including BWAs (NIOSH, 2002). Ventilation systems can also reduce the concentration of particles introduced from air entering a building through filtration. Particle deposition in HVAC systems influences particle concentrations within buildings (Sippola, 2002). Understanding spore aerosol deposition in HVAC ducts is important to help plan incident responses and facility remediation following an attack. The dry, powdered surrogate spores prepared in this study to mimic a typical BWA preparation provide useful data for comparison with other studies based on nonbiological particles, such as latex spheres. The 1-μm fluidized spores used in this study may also provide useful data for BWA transport models.

4.1. *Deposition velocity*

Typical particle disseminations may range from 5 to 20% efficiency. In our tests using galvanized steel or fiberglass ducts, the calculated total

Table 9. Duct surface roughness

Parameter	Plastic micro-structure	Plastic macro-structure	Steel micro-structure	Steel macro-structure	Fiberglass
Description	Internal surface	Folds in film	Internal surface	Horizontal connection seam	Internal surface
Wall roughness, k (cm)	0.0005	0.1–0.3	0.015	0.3–0.4	0.15
Dimensionless roughness, k^+	0.04	9, 6–29	1.2	29–38	12

Table 10. Values for comparison with theoretical deposition models

Parameter	Value
Particle diameter	0.91×10^{-6} cm
Particle density	1.2 g/cm^3
Cunningham slip correction	1.18
Particle dimensionless relaxation time	4.9×10^{-3}
Reynolds number	26,000
Friction factor	6.2×10^{-3}
Friction velocity	14.4 cm/s
Air density	1.2×10^{-3} g/cm^3
Viscosity	1.82×10^{-4} dyne-s/cm^2
Temperature	293 K
Mean free path	6.53×10^{-6} cm
Dimensionless roughness	See Table 9

dissemination efficiencies were typically 9–12%. Once spores were aerosolized, the losses in the once-through system were predicted to be nondetectable for 1-μm spore particles. The geometry of our duct system included vertical rises and angles that likely contributed to the reduction of airborne spores. Spore losses are known to occur in several areas of an HVAC system including cooling coils and angles and corners within a duct system. Other researchers have suggested that, in a standard mechanically ventilated building, reductions of up to 40% of airborne spores may be possible (Fisk, 1994; Seigel and Walker, 2001; Kowalski, 2002).

Deposition velocities of spores in this study were determined by directly measuring the number of viable spores deposited on duct surfaces. A technique that involves counting viable spores may slightly underestimate the total number of spores actually deposited because of the presence of nonviable or nonculturable spores. Enumeration problems are also associated with the surface-sampling technique. Spore extraction from surfaces can vary with the surface material and the sampling method used. Viable spore-counting methods were used in our study because they provide the most important number for estimating human health effects. In addition, the spore preparation used was a reasonable simulant for anthrax BWA. In all tests, we found a significant difference between environmental background microbial counts and the spore deposition data for each of the three duct materials. Deposition velocities for steel (average = 0.16 cm/s) and fiberglass (average = 0.07 cm/s) ducts are within the range of values reported by other researchers using different experimental methods and particles. More specifically, deposition velocities were reported elsewhere to be 0.005 and 0.067 cm/s for particles up to 15 μm in size (Sinclair et al., 1992); 0.005 and 0.43 cm/s for particles 6–9 μm in size (Raunemaa et al., 1989); and calculated to be 0.017 and 0.019 cm/s for particles 1–2 μm in diameter (Thacher and Layton, 1995). Thus, for steel duct, the experimental deposition velocity was about ten times greater than previously reported. For tests using plastic duct, the experimentally determined deposition velocities (0.44–2.4 cm/s) were even greater than results for steel and fiberglass duct.

We found large differences between the deposition velocity onto plastic duct compared to those velocities for steel and fiberglass ducts. This important finding implies that building contamination will likely vary, depending on the type of duct used throughout an affected area.

4.2. *Duct physical properties that influence spore deposition*

Many factors affect potential particle deposition in HVAC systems. Particles may be deposited onto and resuspended from duct surfaces at different rates, depending on particle size, velocity, physical configuration, duct surface, and other environmental factors, such as humidity, dirt, and biofilm formation. Ventilation duct materials containing internal fibrous insulation or residual manufacturing byproducts may also affect the deposition and reaerosolization potential of spores.

Physical parameters, such as roughness of the internal surface and electrical charge of the material, can make a difference in spore deposition velocity. The microscale roughness of the interior surface of materials may also influence the spore deposition rates in ventilation ducts. For example, the rough character of fiberglass is likely to influence particle deposition rates. Several authors have corroborated theoretical models that predict the rate of deposition on rough surfaces is greater than that on smooth surfaces, such as galvanized steel (El-Shobokshy and Ismail, 1979; Fan and Ahmadi, 1995; Sippola, 2002). Our

internally insulated fiberglass duct had a rough surface with fiber depth variation of up to 1.5 mm. Spores may have settled on and adhered to the fibers. Another study using monodisperse experimental particles (diameters = 1, 3, 5, 9, and 16 μm) tagged with a fluorescent tracer found that deposition was much greater in internally insulated ducts than in uninsulated steel ducts (Sippola, 2002). In our experiments, the deposition of 1-μm-diameter spores did not result in a significant difference in counts of spores deposited onto fiberglass versus steel duct surfaces. Particles have been observed in another study to deposit in a nearly uniform manner within insulated ducts with turbulent airflows (Sippola, 2002). That study concluded that the roughness of insulated duct was a dominant factor in deposition.

For the 50-cm circumference of the steel duct we tested, the seam involved only 1.5 cm, or 3% of the total surface area. Only a relatively small proportion of the steel duct surface area had a rough surface (>5, a unitless dimension of roughness). In the case of our flexible plastic duct, the internal surface was predominately covered with folds in the film surrounding the wire helix. Thus, the plastic duct may be considered, in large part, to have a roughness >5. In this study, there was less than a half-log difference between fiberglass and steel duct deposition velocities, with the deposition to the steel surface being greater but statistically insignificant. It is possible that spores adhered to the fiberglass tightly, and our sampling method was insufficient to dislodge the spores. However, use of a surfactant in the sample collection media, and the mechanical action of both sonication and vortexing, should have resulted in spore removal from the insulated fiberglass. A comparison of spore counts between coupon samples and wet-swab samples of steel and plastic provided evidence that the difference between the sampling techniques did not influence the results of this study. A field trial of this nature generally has large experimental errors that include variations in the manufactured duct materials, sampling and analysis, spore viability, and environmental influences.

The greatest deposition velocity we observed was in the flexible plastic duct, which was approximately ten-fold greater than that observed for the steel duct. The flexible plastic duct material used in this study was nonporous, but the internal surface had many small folds that could catch spore particles. Dominant factors affecting the deposition velocity in our study may be the static charge attraction between spores and the plastic duct, the macro-roughness of folds in the plastic film, the wire-helix in the plastic duct, or the joint-seam and corrugated connectors in galvanized steel. We found a difference of two orders of magnitude between the charge of plastic versus that of fiberglass and steel. The static charge from plastic was negative and may have attracted the positively charged spores.

Because all duct materials used in this study were newly supplied from manufacturers, aging effects of dust and biofilm buildup were not considered. However, such effects may have an important impact on spore deposition velocity. Future studies should include an analysis of spore deposition rates in used or aged ducts to determine such effects. Static measurement at the initial time of dissemination may be different from the charge of spores or duct material over a period of time. In terms of decontamination and restoration, it is important to understand the static environments of a building as well as the physical properties of building materials.

4.3. *Dimensionless relaxation time compared to three models*

Deposition velocities resulting from our study were bounded by the three models when comparisons were made with the rough surface (dimensionless roughness, $k^+ = 10$) curves of the models (El-Shobokshy and Ismail, 1979; Wood, 1981; Fan and Ahmadi, 1995).

Our deposition velocities were 10–100 times greater than the velocities predicted for ducts with smoother surfaces, $k^+ = 0.1$. For plastic duct, greater dimensionless deposition velocities were likely the result of charge forces between spores and surface. However, for the steel duct, a relatively large dimensionless deposition velocity was unexpected. Because both galvanized steel and fiberglass duct materials are neutrally charged, and the surface roughness is much greater in fiberglass, the deposition velocity in fiberglass should be greater than that in galvanized steel. The lower spore deposition we observed on

fiberglass is most likely a result of the proprietary biocide used in the acrylic polymer coating. As a result, spores possibly present in numbers would not have grown due to inhibition. These findings imply that building contamination will likely vary, depending on the specific type of duct material used throughout an affected area.

Acknowledgements

The authors wish to thank Don Schwartz, Joe Shinn, John Van Fossen, Souheil Ezzedine, and Kent Wilson. Work was performed under the auspices of the U.S. Department of Energy by Lawrence Livermore National Laboratory under Contract W-7405-ENG-48.

References

Atlas R.M.: 2001, Bioterrorism before and after September 11. *Crit. Rev. Microbiol.* **27**(4): 335–379.

Clesceri, L.S., Greenberg, A.E. & Trussell, R.R. (eds): 1989, *Standard Methods for the Examination of Water and Wastewater*, 17 ed. American Public Health Association: Washington DC.

El-Shobokshy M.S. and Ismail I.A.: 1979, Deposition of aerosol particles from turbulent flow onto rough pipe wall. *Atmos. Environ.* **14**, 297–304.

Fan F.-G. and Ahmadi G.: 1995, A sublayer model for wall deposition of ellipsoidal particles in turbulent streams. *J. Aerosol Sci.* **5**, 813–840.

Fisk W.: 1994, The California healthy buildings study. *Center for Building Science News* **7**, 13.

Fuchs N.A.: 1964, *The Mechanics of Aerosols*, in C.N. Davies (ed.), MacMillan: New York.

Gilchrist M.J.R.: 1992, Microbiological culturing of environmental and medical-device surfaces, in H. Eisenberg (eds), *Clinical Microbiology Procedures Handbook*. American Society for Microbiology: Washington DC, pp. 4–11.

http://www.svce.ac.in/~msubbu/FM-WebBook/Unit-II/VelocityDistributionTurbulent.htm.

Kowalski W.J.: 2002, *Immune Building Systems Technology*, McGraw-Hill: New York ISBN 0-07-140246-2.

Lai A.C.K. and Nazaroff W.W.: 2000, Modeling indoor particle deposition from turbulent flow onto smooth surfaces. *J. Aerosol Sci.* **31**, 463–476.

Matsumoto G.: 2003, Anthrax powder: state of the art?. *Science* **302**, 1492–1497.

National Institute for Occupational Safety and Health (NIOSH): 2002, Guidance for protecting building environments from airborne chemical, biological, or radiological attacks, Department of Health and Human Services, Centers for Disease Control and Prevention, NIOSH Publication No. 2002–139; Cincinnati, OH.

Raunemaa T., Kulmala M., Saari J., Olin M. and Kulamala M.H.: 1989, Indoor air aerosol model transport indoors and deposition of fine and coarse particles. *Aerosol Sci. Technol.* **11**, 11–25.

Rose L., Jensen B., Peterson A., Banerjee S.N. and Arduino M.J.: 2004, Swab materials and *Bacillus anthracis* spore recovery from nonporous surfaces. *Emerg. Infect. Dis.* [serial on the Internet] 2004 June. http://www.cdc.gov/ncidod/EID/vol10no6/03–0716.htm.

Sanderson W.T., Hein M.J., Taylor L., Curwin B.D., Kinnes G.M. and Seitz T.A.: 2002, Surface sampling methods for *Bacillus anthracis* endospore contamination. *Emerg. Infect. Dis.* **8**, 1145–1151.

Schmel G.A.: 1973, Particle eddy diffusivities and deposition velocities for isothermal flow and smooth surfaces. *Aerosol Sci.* **4**, 125–138.

Seigel J.A. and Walker I.S.: 2001, *Deposition of Biological Aerosols on HVAC Heat Exchangers*, Lawrence Berkley National Laboratory: LBNL-47476, Berkeley, CA.

Sextro R.G., Lorenzetti D.M., Sohn M.D. and Thatcher T.L.: 2002, Modeling the spread of anthrax in buildings, *Proceedings Indoor Air 2002 Conference*, pp. 506–511.

Sinclair J.D., Psota-Kelty L.A., Peins G.A. and Ibidunni A.O.: 1992, Indoor/outdoor relationships of airborne ionic substances: comparison of electronic equipment room and factory environments. *Atmos. Environ.* **26A**, 871–882.

Sippola M.R.: 2002, Particle deposition in ventilation ducts, Ph.D. dissertation, University of California, Berkeley, CA, LBNL-52189.

Sippola M.R. and Nazaroff W.W.: 2002, *Particle Deposition from Turbulent Flow: Review of Published Research and its Applicability to Ventilation Ducts in Commercial Buildings*, Lawrence Berkeley National Laboratory, Berkeley, CA, LBNL-51432.

Thacher T.L. and Layton D.W.: 1995, Deposition, resuspension, and penetration of particles within a residence. *Atmos. Environ.* **29**, 1487–1497.

Thacher T.L., Lai A.C.K. and Moreno-Jackson R.: 2002, Effects of room furnishings and air speed on particle deposition rates indoors. *Atmos. Environ.* **36**, 1811–1819.

ThermoAndersen: *Operator Manual: Viable Particle Sizing Sampler*, ThermoAndersen, Smyrna, GA.

U.S. EPA: September 2002, Challenges faced during the Environmental Protection Agency's response to anthrax and recommendations for enhancing response capabilities. A lessons learned report, prepared by the U. S. Environmental Protection Agency.

Wallace L.: 1996, Indoor particles: a review. *J. Air Waste Manage. Assoc.* **46**, 98–126.

Weis C.P., Intrepido A.J., Miller A.K., Cowin P.G., Durno M.A., Gebhardt J.S. and Bull R.: 2003, Secondary aerosolization of viable *Bacillus anthracis* spores in a contaminated US Senate Office. *J. Am. Med. Assoc.* **288**, 2853–2858.

Wood N.B.: 1981, A simple method for the calculation of turbulent deposition to smooth and rough surfaces. *J. Aerosol Sci.* **12**, 275–290.